

Radical Cation Salts with the Nonplanar $[\text{ReO}(\text{dmit})_2]^-$ Complex

Benoît Domercq^[a] and Marc Fourmigué*^[a]

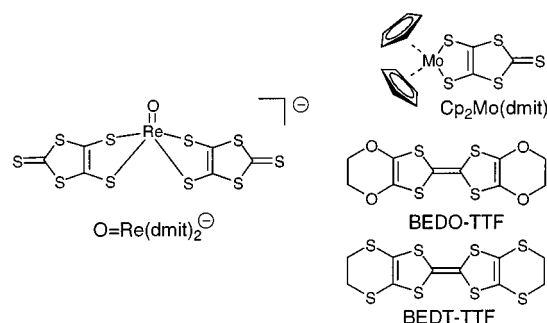
Keywords: S ligands / Rhenium / Oxo complexes / Magnetic properties / Radical ions

An optimized synthesis of $[\text{PPh}_4][\text{ReO}(\text{dmit})_2]$ ($\text{dmit}^{2-} = 2$ -thioxo-1,3-dithiole-4,5-dithiolato) is reported as well as electrocrystallization experiments of various donor molecules with this electrolyte. Three 1:1 salts have been obtained with $\text{Cp}_2\text{Mo}(\text{dmit})$, BEDT-TTF [BEDT-TTF = bis(ethylenedithio)tetrathiafulvalene] and BEDO-TTF [BEDO-TTF = bis(ethylene-dioxo)tetrathiafulvalene] and their X-ray crystal structures

determined. In the three salts, the closed-shell, d^2 , $[\text{ReO}(\text{dmit})_2]^-$ anions push apart the radical cations, stabilizing structures with noninteracting donors [with $\text{Cp}_2\text{Mo}(\text{dmit})$] or donor dimers (with BEDT-TTF or BEDO-TTF), as confirmed by conductivity and SQUID magnetic susceptibility measurements.

Introduction

Planar bis(dithiolene) complexes, and particularly with the sulfur-rich dmit^{2-} ligand, have been extensively used for the elaboration of conducting molecular materials,^[1,2] as, for example, the mixed-valence salts derived from $\text{Ni}(\text{dmit})_2^-$, $[\text{TTF}][\text{Ni}(\text{dmit})_2]_2$ with the open-shell $\text{TTF}^{+\cdot}$ counter cation,^[3] or $[\text{NMe}_4][\text{Ni}(\text{dmit})_2]_2$ with the closed shell NMe_4^+ ammonium cation,^[4] both of them reported to become superconductors. On the other hand, their nonplanar tris(dithiolene) analogs such as $[\text{Mo}(\text{dmit})_3]^-$ or $[\text{V}(\text{dddt})_3]^-$ have been scarcely investigated for the elaboration of conducting salts,^[5,6] probably because their more spherical shape hinders a proper overlap interaction network in the solid state. In this respect, heteroleptic complexes with one of the three dithiolene ligands replaced by a smaller one, such as an oxo or a nitrido group, offer an attractive alternative since more compact structures can be anticipated. Several of those heteroleptic complexes have been described with the dmit^{2-} ligand, some of them diamagnetic (d^2), such as $[\text{MoO}(\text{dmit})_2]^{2-}$,^[7,8] $[\text{ReO}(\text{dmit})_2]^-$,^[9] $[\text{TcN}(\text{dmit})_2]^{2-}$,^[10] and $[\text{OsN}(\text{dmit})_2]^-$ ^[11] and some of them paramagnetic (d^1), such as $[\text{VO}(\text{dmit})_2]^{2-}$ ^[12] or $[\text{MoO}(\text{dmit})_2]^-$.^[7,8] Among these compounds, only $[\text{MoO}(\text{dmit})_2]^-$ forms cation radical salts with TTF to afford a 1:1 salt, $[\text{TTF}][\text{MoO}(\text{dmit})_2]$ which was not structurally characterized.^[8] We therefore decided to investigate more closely the cation radical salts derived from those heteroleptic dithiolene oxo complexes, and present here our results with the closed-shell, diamagnetic Re^{V} $[\text{ReO}(\text{dmit})_2]^-$ anion (Scheme 1). Planar donor molecules such as BEDT-TTF or BEDO-TTF were engaged in electrocrystallization experiments with $[\text{ReO}(\text{dmit})_2]^-$ as well as the nonplanar Mo^{IV} molybdenum complex, $\text{Cp}_2\text{Mo}(\text{dmit})$



Scheme 1

(Scheme 1),^[13] which has been described to be readily oxidized to the corresponding $[\text{Cp}_2\text{Mo}(\text{dmit})]^{+\cdot}$ radical cation.^[14–16]

Results and Discussion

Synthesis

The preparation of $[\text{ReO}(\text{dmit})_2]^-$ has been described by Matsubayashi from the reaction of ReCl_5 with two equivalents of dmit^{2-} in EtOH .^[9] The uncontrolled partial hydrolysis of ReCl_5 under those conditions gave the desired anion in only 30% yield, while a similar reaction in anhydrous CH_3CN gave the homoleptic $[\text{Re}(\text{dmit})_3]^-$ dithiolene complex. We felt that a higher yield could be obtained by using a preformed ReOX_4 moiety, as described for the synthesis^[17] of $[\text{ReO}(\text{mnt})_2]^-$ or $[\text{ReO}(\text{S}_2\text{C}_2\text{B}_{10}\text{H}_{10})_2]^-$,^[18] and chose accordingly to engage the ReOBr_4^- anion, as its tetraphenylphosphonium salt,^[19] in a substitution reaction with two equivalents of dmit^{2-} , affording $[\text{PPh}_4][\text{ReO}(\text{dmit})_2]$ in very good yield (88%) after recrystallization, and identical in every respect to the described compound.^[9]

Structure and Electronic Properties of the $[\text{ReO}(\text{dmit})_2]^-$ Cation Radical Salts

The electrocrystallization of $\text{Cp}_2\text{Mo}(\text{dmit})$, BEDT-TTF and BEDO-TTF in the presence of $[\text{PPh}_4][\text{ReO}(\text{dmit})_2]$ as electrolyte allowed the isolation of the three corresponding

^[a] Sciences Moléculaires aux Interfaces, FRE 2068 CNRS, Institut des Matériaux Jean Rouxel, 2, Rue de la Houssinière, BP32229, 44322 Nantes, France

1:1 salts. $[\text{Cp}_2\text{Mo}(\text{dmit})][\text{ReO}(\text{dmit})_2]$ crystallizes in the monoclinic system, space group $P2_1/c$, with both cation and anion in general positions in the unit cell (Figure 1).

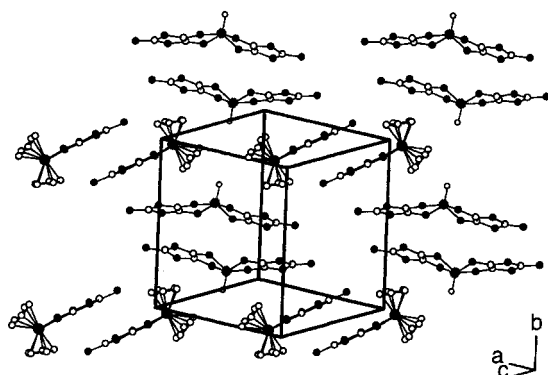


Figure 1. A view of the mixed cation-anion ($a + c$, b) layer in $[\text{Cp}_2\text{Mo}(\text{dmit})][\text{ReO}(\text{dmit})_2]$

The geometry of the $[\text{ReO}(\text{dmit})_2]^-$ anion (Figure 2) is very close to that described for its PPh_4^+ salt (Table 1), although the folding angles of the two ReS_2C_2 metallacycles slightly increase from $11\text{--}15^\circ$ to 17° . Bond length evolution within the organometallic cation (Table 2) confirms the oxidized character of the complex, which changes to a more dithioketonic-type structure for the dithiolene ligand (shortening of the C–S bonds and lengthening of the C=C bond). Note also the weak folding angle θ of the MoS_2C_2 metallacycle along the $\text{S}\cdots\text{S}$ axis in $\text{Cp}_2\text{Mo}(\text{dmit})^{++}$ [$5.6(5)^\circ$] which should be compared to the distortions observed in $[\text{Cp}_2\text{Mo}(\text{dmit})][\text{TCNQF}_4]$ [$\theta = 10.2(1)^\circ$]^[14] while a fully planar metallacycle was observed in $[\text{Cp}_2\text{Mo}(\text{dmit})][\text{AsF}_6]$ ($\theta = 0.0^\circ$).^[15] The cations are organized into inversion-related dimers with a somewhat large interplanar dmit/dmit distance of 3.58 \AA , associated with a lateral offset of 5.51

\AA . Those dimers organize into layers in the (a, c) plane, separated from each other by the diamagnetic $\text{ReO}(\text{dmit})_2^-$ anions. As a consequence of the weakly interacting radical cations, the closed-shell character of the anion and the full charge-transfer, the salt is insulating with $\sigma_{\text{RT}} = 4 \times 10^{-7}\text{ S cm}^{-1}$. Its magnetic behavior was deduced from the SQUID susceptibility measurements which show a Curie–Weiss behavior in the whole temperature range with $\theta = 0.3\text{ K}$, excluding the possibility of sizeable intermolecular interactions in this salt. $[\text{Cp}_2\text{Mo}(\text{dmit})][\text{ReO}(\text{dmit})_2]$ can therefore be described as paramagnetic $[\text{Cp}_2\text{Mo}(\text{dmit})]^{++}$ radical cations, essentially isolated from each other by the closed-shell $[\text{ReO}(\text{dmit})_2]^-$ anions. The situation is more complex in the BEDT-TTF and BEDO-TTT salts.

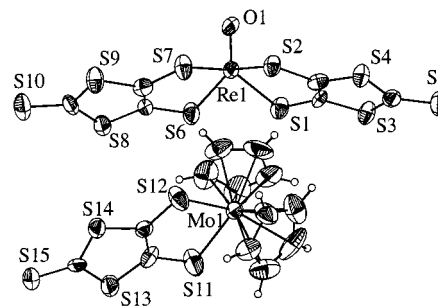


Figure 2. ORTEP view of the $[\text{Cp}_2\text{Mo}(\text{dmit})]^{++}$ cation and the $[\text{ReO}(\text{dmit})_2]^-$ anion in $[\text{Cp}_2\text{Mo}(\text{dmit})][\text{ReO}(\text{dmit})_2]$; thermal ellipsoids at the 50% probability level

$[\text{BEDT-TTF}][\text{ReO}(\text{dmit})_2]$ crystallizes in the monoclinic system, space group $P2_1/n$, with both anion and cation in general positions in the unit cell (Figure 3). The bond lengths within the $[\text{ReO}(\text{dmit})_2]^-$ are similar to those observed above (Table 1). Within the BEDT-TTF moieties, the bond length evolution relative to the neutral molecules con-

Table 1. Geometrical characteristics of the $[\text{ReO}(\text{dmit})_2]^-$ with the different counter ions

Counter ion	PPh_4^+ [9]	$[\text{Cp}_2\text{Mo}(\text{dmit})]^{++}$	BEDT-TTF^{++}	BEDO-TTF^{++}
$\text{Re}-\text{O}/\text{\AA}$	1.687(10)	1.664(8)	1.681(7)	1.655(11)
$\text{Re}-\text{S}/\text{\AA}$	2.332–2.336(5)	2.297–2.320(3)	2.310–2.331(3)	2.309–2.323(4)
$\text{O}-\text{Re}-\text{S}/^\circ$	107.2–109.3(4)	106.3–109.4(3)	105.1–110.7(3)	106.6–109.2(4)
$\text{S}-\text{Re}-\text{S}_{\text{intra}}/\text{ligand}$	83.4(1), 86.6(1)	85.9(1), 86.4(1)	86.5(1), 86.24(9)	85.95–86.44(5)
$\text{S}-\text{Re}-\text{S}_{\text{inter}}/\text{ligand}$	81.0(1), 83.4(1)	82.6(1), 82.9(1)	84.3(1), 83.0(1)	81.77–84.03(5)
folding angles	11.4(4), 14.8(4)	17.6(3), 17.7(1)	23.0(3), 20.1(3)	16.5(4), 18.8(3) 19.8(3), 21.2(4)

Table 2. Geometrical characteristics of $[\text{Cp}_2\text{Mo}(\text{dmit})]^{++}$ in $[\text{Cp}_2\text{Mo}(\text{dmit})][\text{ReO}(\text{dmit})_2]$ together with data for the reference compounds $\text{Cp}_2\text{Mo}(\text{dmit})$ and $[\text{Cp}_2\text{Mo}(\text{dmit})][\text{AsF}_6]$

	$\text{Cp}_2\text{Mo}(\text{dmit})$ neutral ^[15]	$[\text{Cp}_2\text{Mo}(\text{dmit})]^{++}$ as AsF_6^- salt ^[16]	$[\text{Cp}_2\text{Mo}(\text{dmit})]^{++}$ as $[\text{ReO}(\text{dmit})_2]^-$ salt
$\text{Mo}-\text{S}(\text{\AA})$	2.459(3), 2.455(3)	2.441(2)	2.436(3), 2.445(4)
$(\text{Mo})\text{S}-\text{C}(\text{\AA})$	1.763(9), 1.728(9)	1.691(8)	1.704(11), 1.672(13)
$\text{C}=\text{C}(\text{\AA})$	1.357(12)	1.41(1)	1.383(16)
$\text{S}-\text{Mo}-\text{S}(^\circ)$	83.95(8)	83.59(8)	83.42(12)
Folding angle $\theta(^\circ)$	4.2(1)	0.0	5.6(5)

firmly the fully oxidized character of the BEDT-TTF⁺⁺ cation radical (Table 3) when compared with reference compounds,^[20,21] hence the formulation [BEDT-TTF]⁺[ReO(dmit)₂][−]. The organic cation radicals are organized into layers parallel to the (a-c, b) plane (Figure 4), separated from each other by the diamagnetic [ReO(dmit)₂][−] counter anions. Within each organic layer (Figure 5), the BEDT⁺⁺ cation radicals arrange into inversion-centered dimers with short S...S distances (3.42–3.78 Å) and a short interplanar plane-to-plane distance (2.72–2.74 Å). Those dimers interact only weakly with their neighbors in the plane through S...S overlap (S...S distances at 3.67 Å) with the sulfur atoms of the outer dithioethylene moieties.

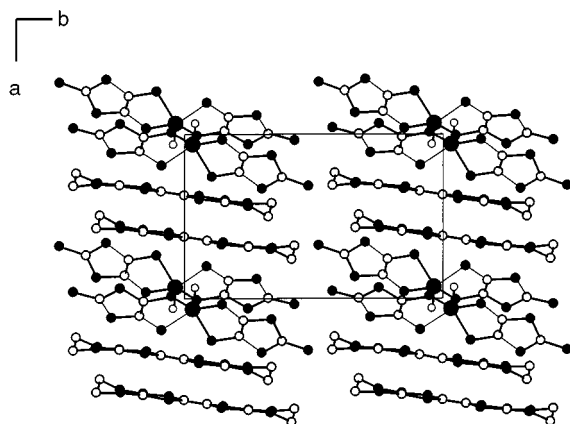
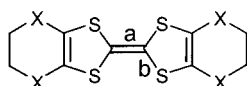


Figure 3. Projection view (along c) of the mixed organic-inorganic layers identified in the structure of [BEDT-TTF][ReO(dmit)₂].

Table 3. Bond length evolution within the TTF core and charge transfer degree (ρ) in BEDT-TTF and BEDO-TTF, in the neutral donor molecules, the two salts with [ReO(dmit)₂][−] and reference salts

				
	ρ	C=C bond (a)	C-S bonds (b)	ref.
BEDT-TTF neutral	0	1.343(3)	1.756(3)	20
[BEDT-TTF][ReO(dmit)]	1	1.397(13)	1.716(11)	this work
BEDT-TTF ⁺⁺ in [BEDT-TTF][PF ₆]	1	1.394(5)	1.722(4)	21
BEDO-TTF neutral	0	1.357(6)	1.761(5)	22
[BEDO-TTF][ReO(dmit)]	1	1.368(10)	1.719(8)	this work
BEDO-TTF ⁺⁺ in [BEDO-TTF][Pd(dto)]	1	1.390(14)	1.729(18)	23

[BEDO-TTF][ReO(dmit)₂], on the other hand, crystallizes in the monoclinic system, space group *P*2₁/*c*, with two crystallographically independent anions and cations in the unit cell. This differentiation originates from different orientations of the ethylenedioxy groups of the BEDO-TTF molecules. The bond lengths within the central TTF core also confirm the oxidized character of the donor molecule (Table 3) when compared with reference compounds.^[22,23]

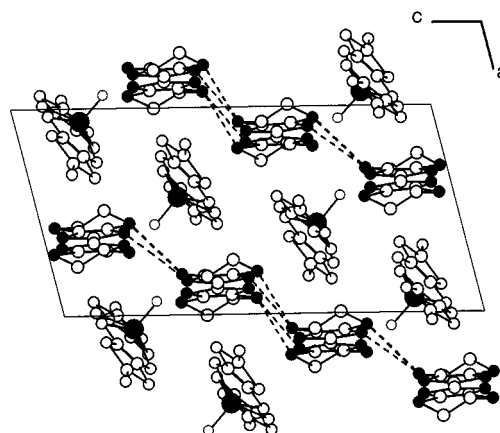


Figure 4. Projection view along b in [BEDT-TTF][ReO(dmit)₂]; the dotted lines indicate the shortest intermolecular S...S contacts between radical BEDT-TTF⁺⁺ moieties; the Re atom and the sulfur atoms of the BEDT-TTF⁺⁺ molecules are shaded

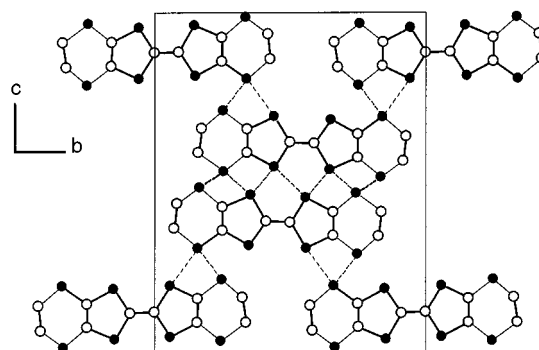


Figure 5. Detail of the intermolecular interaction network between organic BEDT-TTF⁺⁺ cation radicals in [BEDT-TTF][ReO(dmit)₂]

A similar dimer organization of the cation radicals is observed with short S...S (3.56–3.67 Å) and S...O (3.35–3.52 Å) intermolecular contacts (Figure 6), while the dimeric entities are fully isolated from each other by the [ReO(dmit)₂][−] counter ions.

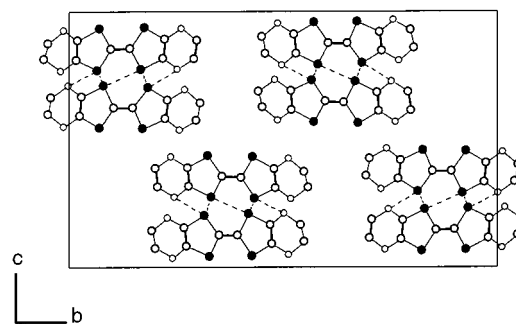


Figure 6. The interaction network identified in the organic layers of BEDO-TTF⁺⁺ cation radicals in the structure of [BEDO-TTF][ReO(dmit)₂]

Conductivity measurements (on compressed pellets) reveal a semi-conducting behavior for both salts with $\sigma_{RT} = 1-3 \times 10^{-6} \text{ S cm}^{-1}$. SQUID measurements of the temperature dependence of the magnetic susceptibility (Figure 7) show, for both salts, an activated behavior in the 100–300 K range together with a Curie tail at low temper-

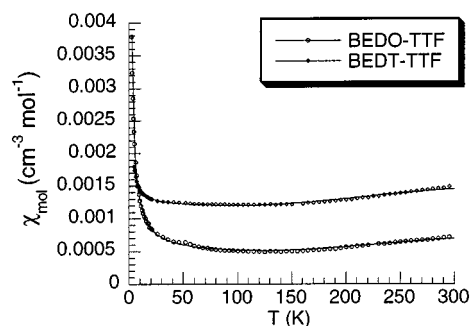


Figure 7. Temperature dependence of the magnetic susceptibility of [BEDT-TTF][ReO(dmit)₂] and [BEDO-TTF][ReO(dmit)₂]; the solid lines are a fit to the singlet-triplet Bleaney–Bower equation with a low-temperature Curie tail (see text)

ature. The latter represents 0.8 and 2.2% $S = 1/2$ magnetic defects in the BEDT-TTF and BEDO-TTF salts respectively. The structural description of these salts indicates the presence of donor dimers, essentially isolated from each other by the diamagnetic anions. The HOMO–HOMO overlap interaction within those dimers leads therefore to bonding and antibonding combinations which house the two remaining electrons. Accordingly, the conductivity is very low and we expect a singlet-triplet magnetic behavior with a maximum for the susceptibility whose temperature $T(\chi_{\max})$ depends upon the HOMO–HOMO interaction energy. The fit of the magnetic susceptibility with the Bleaney–Bower equation,^[24] together with the Curie law encompassing the magnetic defects identified at low temperature, affords J/k values of $-826(5)$ and $-880(7)$ K for the BEDT-TTF and BEDO-TTF salts, respectively. The

close proximity of those two values is indeed in agreement with the extended-Hückel calculated HOMO–HOMO interaction energies within the dimers, which amount to 0.408 and 0.411 eV in the two salts.

Contrary to the situation encountered in organic conductors based on BEDT-TTF or BEDO-TTF, which is characterized by a two-dimensional segregation of the organic donor molecules and the counter ions, we observed here the formation of mixed cationic/anionic layers with the diamagnetic [ReO(dmit)₂][−] units interspersed between the oxidized donor molecules, thus hindering the stabilization of mixed valence, a prerequisite for metallic conductivity. The peculiar alternated structures observed here might be of interest for their magnetic properties, particularly if the diamagnetic [ReO(dmit)₂][−] could be replaced by analogous paramagnetic complexes such as the unknown [MoO(dmit)₂][−] or [ReN(dmit)][−]. Preliminary experiments along those lines showed that ferricinium oxidation of the dianionic [MoO(dmit)₂]^{2−} described by Matsubayashi^[7,8] afforded a bimetallic [Mo₂O₂(μ-O)₂(dmit)₂]^{2−} complex^[25] rather than the expected [MoO(dmit)₂][−].

Table 4. Electrocrystallization conditions

Donor molecule	Cp ₂ Mo(dmit)	BEDT-TTF	BEDO-TTF
m(donor)	5 mg	10 mg	5 mg
m(electrolyte)	500 mg	50 mg	10 mg
V (CH ₂ Cl ₂)	20 mL	15 mL	15 mL
Current intensity	1 μA	1.4 μA	1 μA
Duration	6 days	10 days	17 days

Table 5. Crystallographic data

	[Cp ₂ Mo(dmit)]·[ReO(dmit) ₂]	[BEDT-TTF]·[ReO(dmit) ₂]	[BEDO-TTF]·[ReO(dmit) ₂]
Formula	C ₁₉ H ₁₀ MoOReS ₁₅	C ₁₆ H ₈ OReS ₁₈	C ₃₂ H ₁₆ O ₁₀ Re ₂ S ₂₈
Mol. wt.	1017.31	979.50	1830.53
Crystal system	Monoclinic	Monoclinic	Monoclinic
Space group	<i>P</i> 2 ₁ / <i>c</i>	<i>P</i> 2 ₁ / <i>n</i>	<i>P</i> 2 ₁ / <i>c</i>
<i>a</i> (Å)	14.4017(16)	9.9655(7)	10.6046(10)
<i>b</i> (Å)	14.7254(14)	15.3502(11)	29.3218(18)
<i>c</i> (Å)	13.9482(15)	19.7371(13)	17.8087(14)
β (°)	93.378(13)	104.130(8)	101.488(10)
<i>V</i> (Å ³)	2952.9(5)	2927.9(4)	5426.6(7)
<i>Z</i>	4	4	4
<i>T</i> (K)	293	293	293
<i>d</i> _{calc} , Mg m ^{−3}	2.288	2.222	2.241
μ, mm ^{−1}	5.6	5.45	5.587
<i>F</i> (000)	1956	1900	3544
Crystal size	0.50×0.04×0.02	0.3×0.1×0.01	0.354×0.04×0.02
θ range	1.98–25.96	1.7–24	1.81–26
Refl. coll.	5732	18364	10575
Refl. ind	5732	4582	10575
<i>R</i> _{int}	0	0.125	0.1740
Abspt. corr.	Numerical	Empirical	Numerical
Max., min. trans.	0.8788, 0.5324	0.6352, 0.4086	0.8641, 0.2888
Data/rest/par.	5732/0/334	4583/0/325	10575/0/649
GOF	0.528	0.753	0.504
<i>R</i> (<i>F</i>), <i>wR</i> (<i>F</i> ²)	0.0414, 0.0979	0.0419, 0.0705	0.0464, 0.1177
Res. dens.	1.96, −1.03	1.25, −0.74	1.25, −0.66

Experimental Section

Synthesis: All reactions were performed under nitrogen using vacuum line techniques. Solvents were dried prior to use. [PPh₄][ReOBr₄] was prepared according to Cotton et al.^[19] in 44.3% yield. — C₂₄H₂₀Br₄OPRe: calcd. C 33.47, H 2.34, Br 37.11, P 3.60; found C 33.72, H 2.39, Br 37.38, P 3.60.

[PPh₄][ReO(dmit)₂]: A solution of dmit(COPh)₂ (0.5 g, 1.23 mmol) in dry MeOH (5 mL) was treated with a MeOH solution of NaOMe (2.1 equiv.). After stirring for 1 h, the dark red solution was precipitated with Et₂O (20 mL), and the red dithiolene salt decanted, washed with Et₂O and dried. Na₂(dmit) was dissolved in MeOH (40 mL) and added dropwise to a solution of [PPh₄][ReOBr₄] (0.5 g, 0.58 mmol) in MeOH (50 mL). A red solid immediately precipitated. After stirring overnight it was filtered and recrystallized from CH₂Cl₂/EtOH, affording 0.48 g (88%) of the salt as dark red crystals. M.p. 224–225 °C. — C₃₀H₂₀OPReS₁₀: calcd. C 38.57, H 2.16, P 3.32, S 34.32; found C 36.18, H 1.98, P 3.71, S 36.15.

Electrocrystallization Experiments: Two-compartment cells with platinum electrodes (l = 2 cm, Ø = 1 mm) were used in the galvanostatic mode at 20 °C. Crystals were harvested on the anode after the indicated time and washed with CH₂Cl₂. Details for each individual compound are given in Table 4.

Data Collection and Structure Determination: Table 5 summarizes the crystallographic data. Data were collected at room temperature on an Imaging Plate Diffraction System (Stoe-IPDS). Structures were solved by direct methods using SHELXS-86 and refined by the full-matrix least-squares method on F², using SHELXL-93 (G. M. Sheldrick, University of Göttingen, 1993) with anisotropic thermal parameters for all non-hydrogen atoms. The hydrogen atoms were introduced at calculated positions (riding model). Crystallographic data (excluding structure factors) for the structures reported in this paper have been deposited with the Cambridge Crystallographic Data Centre as supplementary publication nos. CCDC-149592–149594 for the Cp₂Mo(dmit), the BEDT-TTF and the BEDO-TTF salts, respectively. Copies of the data can be obtained free of charge on application to CCDC, 12 Union road, Cambridge CB2 1EZ, UK [Fax: (internat.) + 44-1223/336-033; E-mail: deposit@ccdc.cam.ac.uk].

Magnetic Measurements: Magnetic susceptibilities were measured on a Quantum Design MPMS-2 SQUID magnetometer operating in the range 2.5–300 K at 1 T ([BEDT-TTF][ReO(dmit)₂], 12.32 mg) or 0.5 T ([BEDO-TTF][ReO(dmit)₂], 6.53 mg). Data were corrected for sample holder contribution and Pascal diamagnetism.

- [1] Reviews on dmit^{2−} complexes have appeared: P. Cassoux, L. Valade, H. Kobayashi, A. Kobayashi, R. A. Clark, A.E. Underhill, *Coord. Chem. Rev.* **1991**, *110*, 115–160.
- [2] R.-M. Olk, B. Olk, W. Dietzsch, R. Kirmse, E. Hoyer, *Coord. Chem. Rev.* **1992**, *117*, 99–131.
- [3] M. Bousseau, L. Valade, J.-P. Legros, P. Cassoux, M. Garbauskas, L. V. Interrante, *J. Am. Chem. Soc.* **1986**, *108*, 1908–1916.
- [4] A. Kobayashi, H. Kim, Y. Sasaki, R. Kato, H. Kobayashi, S. Morinaga, Y. Nishino, K. Kajita, T. Tanaka, *Chem. Lett.* **1987**, 1819–1822.
- [5] G. Matsubayashi, K. Douki, H. Tamura, M. Nakano, W. Mori, *Inorg. Chem.* **1993**, *32*, 5990–5996.
- [6] C. Livage, M. Fourmigué, P. Batail, E. Canadell, C. Coulon, *Bull. Soc. Chim. Fr.* **1993**, *130*, 761–771.
- [7] G. Matsubayashi, T. Nojo, T. Tanaka, *Inorg. Chim. Acta* **1988**, *154*, 133–135.
- [8] T. Nojo, G. Matsubayashi, T. Tanaka, *Inorg. Chim. Acta* **1989**, *159*, 49–53.
- [9] G. Matsubayashi, T. Maikawa, M. Nakano, *J. Chem. Soc., Dalton Trans.* **1993**, 2995–2999.
- [10] J. R. Dilworth, R. Hübener, U. Abram, *Z. Anorg. Allg. Chem.* **1997**, *623*, 880–882.
- [11] W. A. Reinert, P. A. Shapley, *Inorg. Chim. Acta* **1998**, *267*, 335–340.
- [12] R. Kirmse, W. Dietzsch, J. Stach, R.-M. Olk, E. Hoyer, *Z. Anorg. Allg. Chem.* **1987**, *548*, 133–140.
- [13] M. Fourmigué, C. Lenoir, C. Coulon, F. Guyon, J. Amaudrut, *Inorg. Chem.* **1995**, *34*, 4979–4985.
- [14] M. Fourmigué, B. Domercq, I. V. Jourdain, P. Molinié, F. Guyon, J. Amaudrut, *Chem. Eur. J.* **1998**, *4*, 1714–1723.
- [15] R. Clérac, M. Fourmigué, J. Gaultier, Y. Barrans, P.-A. Albouy, C. Coulon, *Eur. Phys. J. B* **1999**, *9*, 431–443.
- [16] B. Domercq, C. Coulon, M. Fourmigué, *Inorg. Chem.* **2001**, *40*, 371–378.
- [17] A. Davison, C. Orvig, H. S. Trop, M. Sohn, B. V. DePhamphilis, A. G. Jones, *Inorg. Chem.* **1980**, *19*, 1988–1992.
- [18] J. D. McKinney, H. Chen, T. A. Hamor, K. Paxton, C. J. Jones, *J. Chem. Soc., Dalton Trans.* **1998**, 2163–2168.
- [19] F. A. Cotton, K. J. Lippard, *Inorg. Chem.* **1966**, *5*, 9–16.
- [20] P. Guionneau, C. J. Kepert, D. Chasseau, M. R. Truter, P. Day, *Synth. Metals* **1997**, *86*, 1973–1974.
- [21] H. Kobayashi, R. Kato, T. Mori, A. Kobayashi, Y. Sasaki, G. Saito, T. Enoki, H. Inokuchi, *Chem. Lett.* **1983**, 759–760.
- [22] T. Suzuki, H. Yamochi, G. Srdanov, K. Hinkelmann, F. Wudl, *J. Am. Chem. Soc.* **1989**, *111*, 3108–3109.
- [23] G. Saito, H. Izukashi, M. Shibata, K. Yoshida, L. A. Kushch, T. Kondo, H. Yamochi, O. O. Drozdova, K. Matsumoto, M. Kusunoki, K. Sakaguchi, N. Kojima, E. B. Yagubskii, *J. Mater. Chem.* **2000**, *10*, 893–910.
- [24] O. Kahn, in *Molecular Magnetism*, VCH, Weinheim, **1993**.
- [25] B. Domercq, PhD thesis, University of Nantes, France, **1999**.

Received September 13, 2000

[I00346]